

# Single Phase Bidirectional H6 Rectifier/Inverter

Jianhua Wang, *Member, IEEE*, Shang Gao, Yichao Sun, *Member, IEEE*, Zhendong Ji, Lexiang Cheng, Lingyu Li, Wei Gu, *Member, IEEE*, Jianfeng Zhao

**Abstract-** Transformer-less photovoltaic (PV) inverters are more widely adopted due to high efficiency, low cost and light weight, etc. However, H5, HERIC, etc. transformer-less PV inverters do not have the bidirectional capability for solar energy storage system in the future. With topology derivation history reviewed from rectifier to inverter, the essence of bidirectional rectifier/inverter is revealed to find a reverse power flow approach. Therefore, this paper proposes an advanced bidirectional technique for a selected H6 inverter topology with only modulation strategy modified, while the others remain the same. For the H6 circuitry in both rectifier and inverter modes, excellent three level DM voltage feature is achieved, while leakage current issue is eliminated at the same time with improved modulation method. Simulations and experimental results verify the proposed single phase bidirectional H6 rectifier/inverter technique.

**Keywords-** H6 inverter; rectifier; improved modulation; bidirectional power flow; leakage current

## I. INTRODUCTION

High penetration installed renewable energies are playing more important roles in electric power system, which gradually change the existing utility grid with more power electronics features due to grid-connected converters[1]. In summer weekends, renewable energies already provide 100% of demand in Germany [2]. The fundamental operation codes for existing power grid are continuously modified for grid-tie inverters, especially for PV applications [3]. The grid codes are not only focusing on unilateral restrictions on leakage current safety, harmonic limits, and anti-islanding requirements, but also place great emphasis on faults ride-through ability, reactive power compensation capability, grid frequency stability, and so on[4]-[17].

Manuscript received August 21, 2018; revised October 15, 2018; accepted January 26, 2019.

This work was supported in part by the Natural Science Foundation of Jiangsu Province (BK20181283), Science and Technology Project of State Grid Jiangsu Electric Power Co. Ltd of China (J2018081), and the Fundamental Research Funds for the Central Universities (No. 2242018K41066). (*Corresponding author: Jianhua Wang*)

Jianhua Wang, Shang Gao, Wei Gu, Jianfeng Zhao are with Jiangsu Provincial Key Laboratory of Smart Grid Technology & Equipment, School of Electrical Engineering, Southeast University, Nanjing, China (email: wangjianhua@seu.edu.cn; 454750523@qq.com; wgu@seu.edu.cn; jianfeng\_zhao@seu.edu.cn).

Yichao Sun is with School of Electrical and Automation Engineering, Nanjing Normal University, Nanjing, China (e-mail: yichao.sun1987@gmail.com).

Zhendong Ji is with Department of Electrical Engineering, School of Automation, Nanjing University of Science and Technology, Nanjing, China (e-mail: zhendong\_ji@126.com).

Lexiang Cheng is with State Grid Nanjing Power Supply Company, Nanjing, China (364202827@qq.com).

Lingyu Li State Grid Yancheng Power Supply Company, Yancheng, China (lilingyu1102@126.com).

Traditional AC grids have a hierarchical structure and designed radial, ignorant to energy feed-in in medium- and low-voltage distribution grids considering regional energy resources balance. However, future grids cannot ignore the energy feed-in in medium- and low-voltage distribution grids. Voltage violation problems caused by high-density distributed PVs are common in distribution grids, which restrict the penetration rate of PV installations. Central static var generator (SVG), or distributed PV inverters with reactive power compensation capability of their own could eliminate voltage exceeding specified limits. The former SVG approach is more suitable for central PV plants, while the latter one would lose the price subsidy based on active power generation.

From the viewpoint of regional energy resources balance, distributed PV installation with energy storage is an attractive solution for high penetration PV applications like that in micro-grids. With the promotion and development of electric vehicles, battery cost would decrease following the similar cost reduction curve of PV products that took place in the past 20 years. A boom in battery industry, and there would be an increase in solar energy storage system. However, at present, most classic transformer-less PV inverters such as H5, HERIC, etc., do not have the bidirectional capability either. Therefore, scholars, scientists, engineers are continuously investigating bi-directional power conversion techniques for solar energy storage system. Novel topologies and control schemes are proposed to bridge the technology gap.

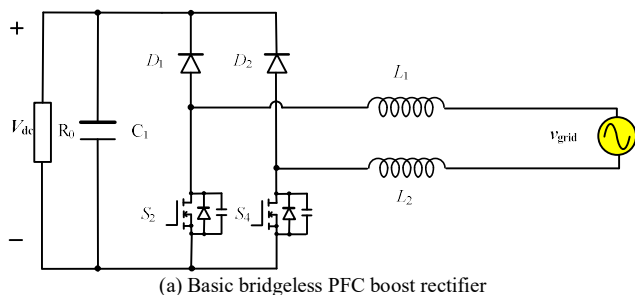
Based on half-bridge cell, a high efficiency dual buck-type inverter along with an admittance-compensated quasi-proportional resonant controller is proposed in [18] to ensure high power quality and precision power flow control. It is a half-bridge-type inverter, and it is more suitable for 110Vac grid considering 650V metal-oxide-semiconductor field-effect transistor (MOSFET) voltage stress. A cascade dual-boost/buck half-bridge converter based on the dual buck-type inverter is proposed for grid-tie transformer-less battery energy storage systems [19], no shoot-through issue is achieved with more units cascaded for high voltage applications. Furthermore, a dual buck-type full bridge bidirectional AC-DC converter is proposed in [20], utilizing two split ac-coupled inductors that operate separately for positive and negative half grid cycles in both inversion and rectification operations. It works as an ac-switch transformer-less inverter like HERIC circuitry in inversion mode and bridgeless power factor corrector (PFC) in rectification mode. The common mode (CM) voltages and associated leakage currents can be minimized in the proposed topology both in inversion and rectification modes. Based on the high-

frequency leg (HFL) technique, Reference [21] further improves the dual buck-type full bridge bidirectional AC-DC converter with discontinuous current mode/continuous current mode operations.

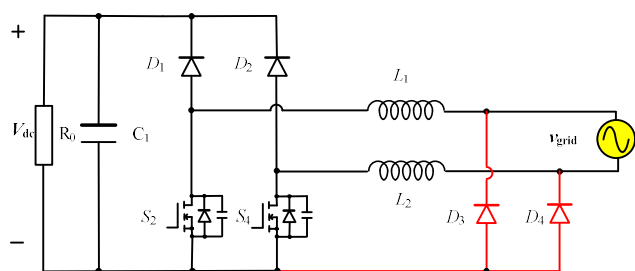
For full-bridge type inverter, classic H5, HERIC, etc. transformer-less PV inverters do not have the bidirectional capability [21]. However, these topologies and derived circuitries such as numerous H6 inverters are the dominant circuits in single phase transformer-less PV applications. Since bidirectional power capability is a challenge to existing H6 inverters, the motivation of this manuscript is to find an advanced solution for them. In this paper, the relationship between bridgeless PFC boost rectifier and transformer-less inverter is reviewed and expounded at first. Then, a novel modulation method is proposed for single phase H6 inverter reform. It not only has bidirectional power flow feature but also retains the existing H6 inverter advantages, e.g. CM voltage and high efficiency. At last, PSIM Simulations and experimental test results verify the proposed single phase bidirectional H6 rectifier/inverter.

## II. THE RELATIONSHIP BETWEEN BRIDGELESS PFC BOOST RECTIFIER AND TRANSFORMER-LESS INVERTER

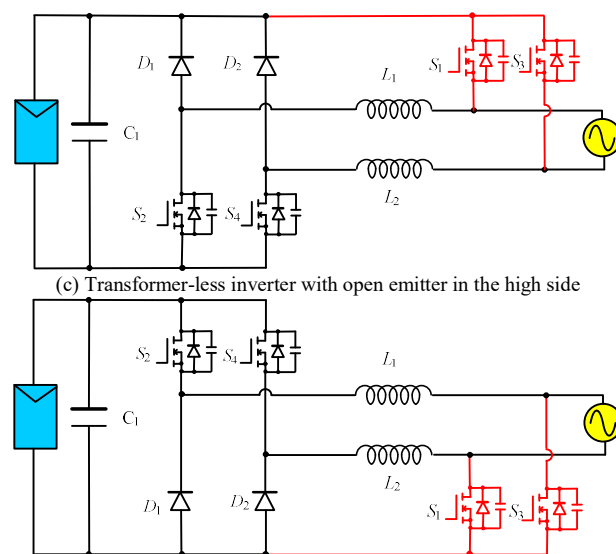
In most cases the boost topology is used for single phase active power factor correction with input diode rectifier. The current have to pass at least 3 semiconductors including 2 diodes. Classic bridgeless PFC boost rectifier using split chokes without the input rectifier for each half-



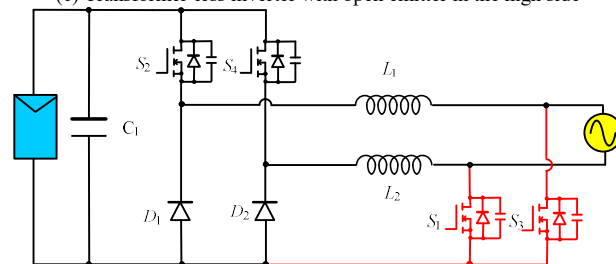
(a) Basic bridgeless PFC boost rectifier



(b) Improved bridgeless PFC boost rectifier



(c) Transformer-less inverter with open emitter in the high side



(d) Improved transformer-less inverter with open emitter in the low side

Figure 1 The relationship between bridgeless PFC boost rectifier and transformer-less inverter

wave in Fig.1 (a) is proposed. The problem is that the connection of both input lines to a PFC choke. The outcome of this is the floating of the output with high frequency relative to input source.

A new topology invented by Temesi Ernő and Michael Frisch in Vincotech does solve the problem [22]. Two chokes with the same inductance as in the standard boost topology are required. But only 1 inductor is used per half wave. The other one is bypassed by additional rectifiers as Fig. 1(b) illustrated. It is interesting to find that 4 years later Michael Frisch and Temesi Ernő also proposed transformer-less inverter with open emitter in the high side in Fig.1(c), which is switched only with 50Hz as  $D_3$ ,  $D_4$  in Fig.1 (b) [23].

Similarly, another transformer-less inverter with open emitter in the low side is proposed in [24] as Fig.1 (d) illustrated. The basic idea behind it is to associate two parallel step-down converters with the output connected to the load using opposite polarities. It is derived from [25], where one of the discussed power-factor correction circuits was modified to get a reverse power flow.

In general, Fig.1 summarizes relationship between bridgeless PFC boost rectifier and transformer-less inverter, the essence of variant circuits is to find a reverse power flow approach, which would help bidirectional rectifier/inverter developed.

## III. SELECTED H6 INVERTER WITH A REVERSE POWER FLOW

### A. Selected H6 Inverter with its corresponding hybrid modulation method

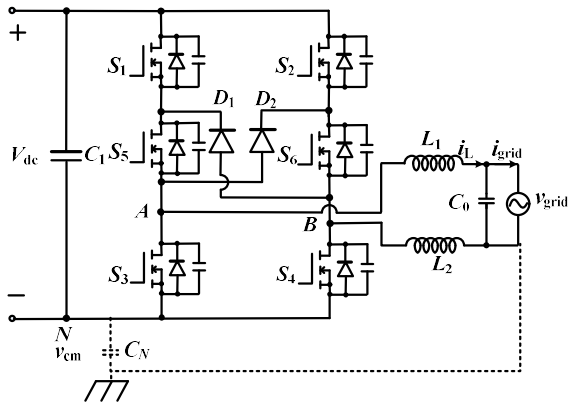


Figure 2 Selected H6 inverter

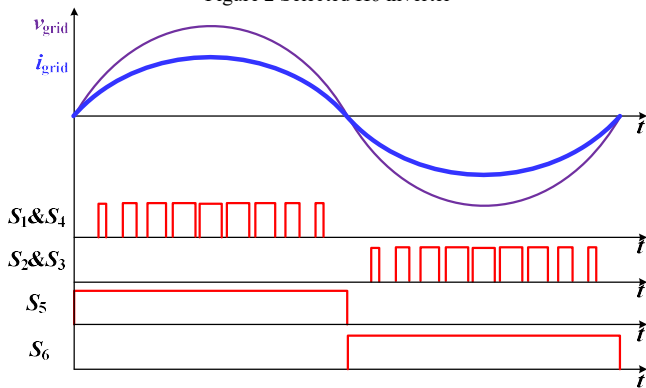
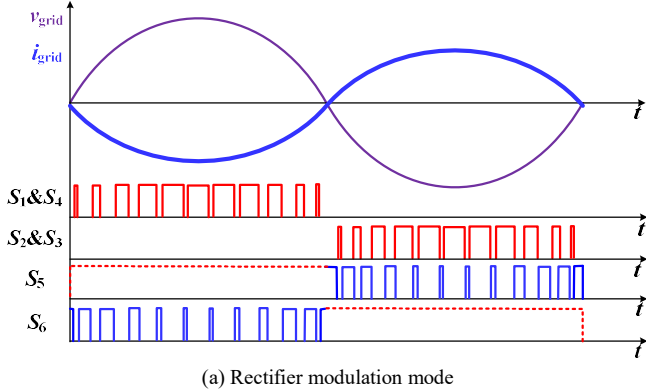


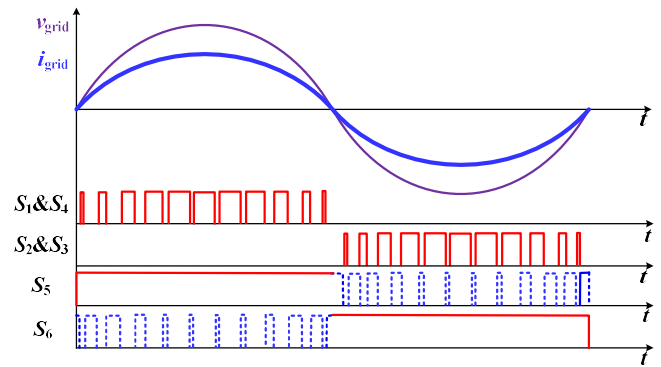
Figure 3 Corresponding hybrid modulation method for the selected H6 inverter

H5, HERIC, and H6 types are the dominant topologies in single phase transformer-less PV inverters. One H6 inverter as Fig.2 shown is selected as an example for further analysis below. Fig.3 further illustrates its corresponding hybrid modulation method for the selected H6 inverter, where intermediate active devices  $S_5$  and  $S_6$  are switched only with line frequency 50/60Hz. The diagonal active devices  $S_1$ ,  $S_4$ , and  $S_2$ ,  $S_3$  are high frequency switches during positive grid cycle or negative grid cycle, respectively. Most of existing literatures about H6 topologies only covers grid-connected applications.

### B. Bidirectional H6 Rectifier/Inverter with novel hybrid modulation method



(a) Rectifier modulation mode



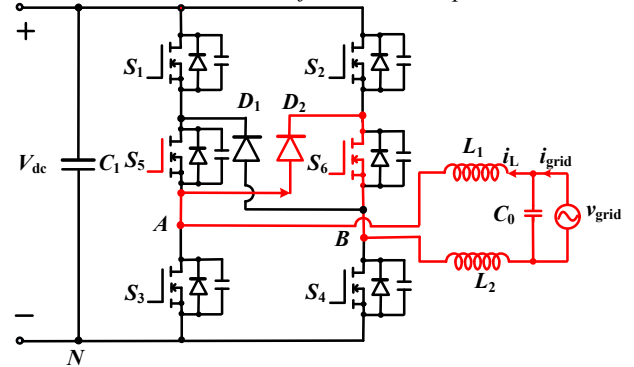
(b) Inverter modulation mode

Figure 4 Novel hybrid modulation method for selected H6 converter

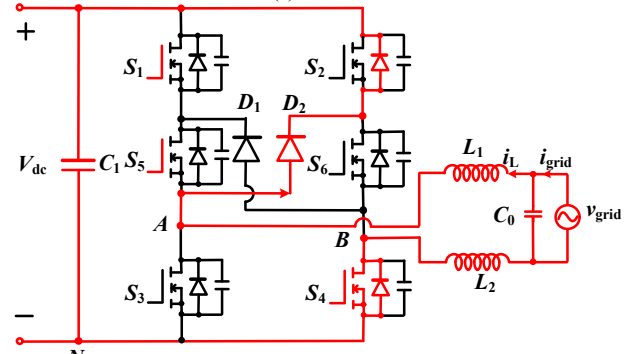
Focusing on energy storage application in the near future, a novel hybrid modulation method is proposed in Fig.4 for the selected bidirectional H6 converter in Fig.2. Fig.4 (a) and Fig.4 (b) shows the rectifier and inverter modulation modes, respectively. It is found that the high frequency switching patterns for  $S_1$ ,  $S_4$ , and  $S_2$ ,  $S_3$  remains the same. During former off mode in Fig.3, line frequency switches  $S_5$ ,  $S_6$  in Fig.4 also switch with high frequency pulses, which are the opposite of  $S_1$ ,  $S_4$ , and  $S_2$ ,  $S_3$ , respectively.

It should be noted that the added high frequency pulses for  $S_5$ ,  $S_6$  are invalid for H6 inverter as Fig.4 (b) illustrated. With additional drive signals applied, the voltages, currents and power flows remain the same as that in Fig.3. Detail operation modes and analysis for Fig.4 are presented in the next section III.C.

### C. Bidirectional H6 Rectifier/Inverter Operation Modes



(a) Mode 1



(b) Mode 2

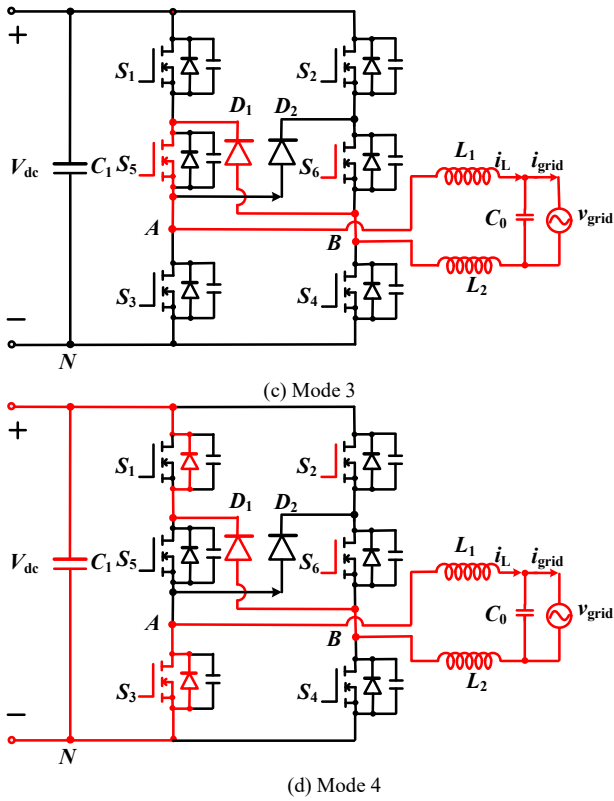


Figure 5 H6 rectifier operation modes

**In H6 rectifier mode 1**, as Fig.5(a) shown, during positive grid cycle while  $S_5$  is always on,  $S_6$  is turned on with high frequency, and grid charges the chokes  $L_1$  and  $L_2$  through a combination of path between grid,  $L_1$ ,  $D_2$ ,  $S_6$ , and  $L_2$ .

Although  $S_5$  is on, no current flow through it. However, with the contribution of shorten  $S_5$ ,  $v_{AN}=0.5V_{dc}$  due to split voltage between deactivated  $S_1$  and  $S_3$ . For the same reason,  $v_{BN}=0.5V_{dc}$ , therefore,

$$\begin{aligned} \text{Differential mode voltage } v_{dm} &= v_{AB} = v_{AN} - v_{BN} = 0 \\ \text{Common mode voltage } v_{cm} &= (v_{AN} + v_{BN})/2 = 0.5V_{dc} \end{aligned} \quad (1)$$

**In H6 rectifier mode 2**, as Fig.5 (b) shown, during positive grid cycle while  $S_5$  is always on,  $S_6$  is turned off with high frequency. With active  $S_1$  and  $S_4$ , continuous inductor current finds the demagnetization path for chokes  $L_1$  and  $L_2$ : grid,  $L_1$ ,  $D_2$ ,  $D_{S2}$ , dc side,  $S_4$  ( $D_{S4}$ ), and  $L_2$ , which is a reverse inner path for bidirectional power flow.

Since  $S_1$  and  $S_5$  are turned on, bridge middle-point A is clamped to dc bus high side, then  $v_{AN} = V_{dc}$ . At the same time, bridge middle-point B is clamped to dc bus low side, therefore,  $v_{BN} = 0$ ,

$$\begin{aligned} v_{dm} &= v_{AB} = v_{AN} - v_{BN} = V_{dc} \\ v_{cm} &= (v_{AN} + v_{BN})/2 = 0.5V_{dc} \end{aligned} \quad (2)$$

**In H6 rectifier mode 3**, as Fig.5(c) shown, during negative grid cycle while  $S_6$  is always on,  $S_5$  is turned on with high frequency, and it is a mirror state as mode 1 illustrated. The reverse power flow loop is a combination of path between grid,  $L_2$ ,  $D_1$ ,  $S_5$ , and  $L_1$ . Similarly,

$$\begin{aligned} v_{dm} &= v_{AB} = v_{AN} - v_{BN} = 0.5V_{dc} - 0.5V_{dc} = 0 \\ v_{cm} &= (v_{AN} + v_{BN})/2 = (0.5V_{dc} + 0.5V_{dc})/2 = 0.5V_{dc} \end{aligned} \quad (3)$$

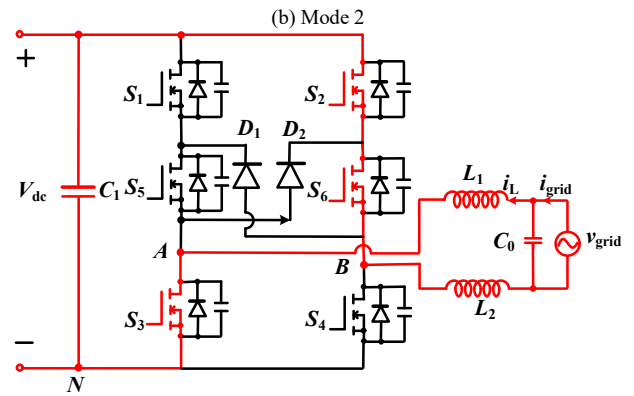
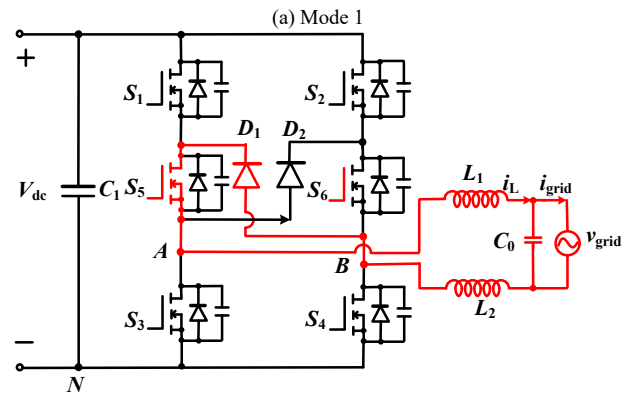
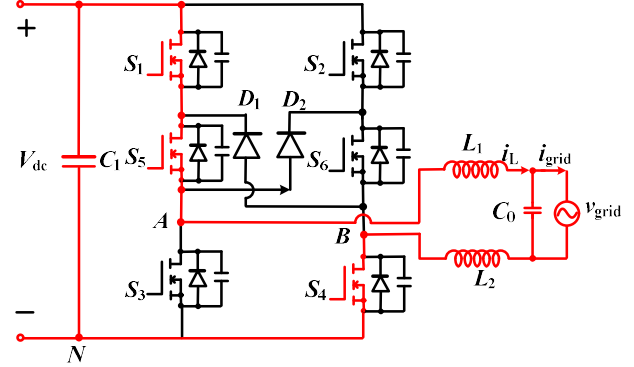
**In H6 rectifier mode 4**, as Fig.5(d) shown, during negative grid cycle while  $S_6$  is always on,  $S_5$  is turned off with high frequency, and it is a mirror state as mode 2 illustrated. Power flow loop is a combination of path between grid,  $L_2$ ,  $D_1$ ,  $D_{S1}$ , dc side,  $S_3$  ( $D_{S3}$ ), and  $L_1$ . Similarly,

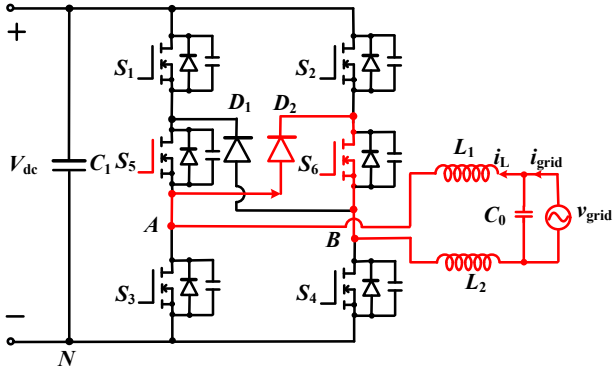
$$\begin{aligned} v_{dm} &= v_{AB} = v_{AN} - v_{BN} = 0 - V_{dc} = -V_{dc} \\ v_{cm} &= (v_{AN} + v_{BN})/2 = (0 + V_{dc})/2 = 0.5V_{dc} \end{aligned} \quad (4)$$

Fig.6 also presents H6 inverter operations modes following modulation mode in Fig.4, detail operations are provided below.

**In H6 inverter mode 1**, as Fig.6(a) shown, during positive grid cycle while  $S_5$  is always on,  $S_1$  and  $S_4$  are turned on synchronously with same high frequency, and dc side charges the chokes  $L_1$ ,  $L_2$ , and grid through a combination of path between  $S_1$ ,  $S_5$ ,  $L_1$ , grid,  $L_2$ ,  $S_4$ .

Since  $S_1$  and  $S_5$  are turned on, bridge middle-point A is





(d) Mode 4

Figure 6 H6 inverter operation modes

clamped to dc bus high side, then  $v_{AN} = V_{dc}$ . At the same time, bridge middle-point B is clamped to dc bus low side, therefore,  $v_{BN} = 0$ ,

Differential mode voltage  $v_{dm} = v_{AB} = v_{AN} - v_{BN} = V_{dc}$

Common mode voltage  $v_{cm} = (v_{AN} + v_{BN})/2 = 0.5V_{dc}$  (5)

**In H6 inverter mode 2**, as Fig.6 (b) shown, during positive grid cycle while  $S_5$  is always on. With deactivated  $S_1$  and  $S_4$ , continuous inductor current finds the freewheeling path for chokes  $L_1$  and  $L_2$ : grid,  $L_2$ ,  $D_1$ ,  $S_5$ , and  $L_2$ .

Although  $S_6$  is turned on with high frequency at this time, no current flow through it. However, with the contribution of shorten  $S_6$ ,  $v_{BN} = 0.5V_{dc}$  due to split voltage between deactivated  $S_2$  and  $S_4$ . For the same reason,  $v_{AN} = 0.5V_{dc}$ , therefore,

$$\begin{aligned} v_{dm} &= v_{AB} = v_{AN} - v_{BN} = 0 \\ v_{cm} &= (v_{AN} + v_{BN})/2 = 0.5V_{dc} \end{aligned} \quad (6)$$

**In H6 inverter mode 3**, as Fig.6(c) shown, during negative grid cycle while  $S_6$  is always on,  $S_2$ ,  $S_3$  are turned on with the high frequency, and it is a mirror state as mode 1 illustrated. The power flow loop is a combination of path between grid,  $L_1$ ,  $S_3$ , dc side,  $S_2$ ,  $S_6$ , and  $L_2$ . Similarly,

$$\begin{aligned} v_{dm} &= v_{AB} = v_{AN} - v_{BN} = 0 - V_{dc} = -V_{dc} \\ v_{cm} &= (v_{AN} + v_{BN})/2 = (0 + V_{dc})/2 = 0.5V_{dc} \end{aligned} \quad (7)$$

**In H6 inverter mode 4**, as Fig.6(d) shown, during negative grid cycle while  $S_6$  is always on,  $S_5$  is turned on with high frequency, and it is a mirror state as mode 2 illustrated. Current Freewheeling loop is a combination of path between grid,  $L_2$ ,  $D_1$ ,  $S_3$ , and  $L_1$ . Similarly,

$$\begin{aligned} v_{dm} &= v_{AB} = v_{AN} - v_{BN} = 0.5V_{dc} - 0.5V_{dc} = 0 \\ v_{cm} &= (v_{AN} + v_{BN})/2 = (0.5V_{dc} + 0.5V_{dc})/2 = 0.5V_{dc} \end{aligned} \quad (8)$$

#### IV. DISCUSSION AND DESIGN CONSIDERATION

##### A. Advanced DM, CM features for bidirectional H6 converter with proposed modulation method

With detail operation modes analyzed in above section III, Tab.1 further summarizes some important features for the bidirectional H6 inverter. It is found that no matter it is a rectifier or inverter, common mode voltage of the bidirectional H6 inverter is almost a constant dc value, which would eliminate inverter's leakage current and improve EMC characteristic of PFC converter.

On the other hand, the differential voltage changes between  $V_{dc}$ , 0, and  $-V_{dc}$ . It is a typical three level voltage, which indicates good power quality of grid side, no matter it is a rectifier or inverter.

##### B. Modulation comparison for bidirectional power flow and unidirectional power flow

In Tab.1, it is found that H6 inverter or traditional modulation method are almost the same. The differences are high frequency switching patterns for with  $S_5$  and  $S_6$  with dashed line in Fig. 4(b). Actually, the dashed switching pulses could also be removed for inverter mode. For the same reason, line frequency switching pulses for with  $S_5$  and  $S_6$  with dashed

TAB.I COMPARISON SUMMARY

Figures	Traditional Hybrid Modulation Method	Improved Hybrid Modulation Method	Corresponding Current paths	Level	
				$v_{cm}$	$v_{dm}$
Figure 5(a)	/	Rectifier Mode 1	grid, $L_1$ , $D_2$ , $S_6$ , and $L_2$	$0.5V_{dc}$	0
Figure 5(b)	/	Rectifier Mode 2	grid, $L_1$ , $D_2$ , $D_{S2}$ , dc side, $S_4$ ( $D_{S4}$ ), and $L_2$	$0.5V_{dc}$	$V_{dc}$
Figure 5(c)	/	Rectifier Mode 3	grid, $L_2$ , $D_1$ , $S_5$ , and $L_1$	$0.5V_{dc}$	0
Figure 5(d)	/	Rectifier Mode 4	grid, $L_2$ , $D_1$ , $D_{S1}$ , dc side, $S_3$ ( $D_{S3}$ ), and $L_1$	$0.5V_{dc}$	$-V_{dc}$
Figure 6(a)	Inverter Mode 1	Inverter Mode 1	$S_1$ , $S_5$ , $L_1$ , grid, $L_2$ , and $S_4$	$0.5V_{dc}$	$V_{dc}$
Figure 6(b)	Inverter Mode 2	Inverter Mode 2	grid, $L_2$ , $D_1$ , $S_5$ , and $L_1$	$0.5V_{dc}$	0
Figure 6(c)	Inverter Mode 3	Inverter Mode 3	grid, $L_1$ , $S_3$ , dc side, $S_2$ , $S_6$ , and $L_2$	$0.5V_{dc}$	$-V_{dc}$
Figure 6(d)	Inverter Mode 4	Inverter Mode 4	grid, $L_2$ , $D_1$ , $S_3$ , and $L_1$	$0.5V_{dc}$	0

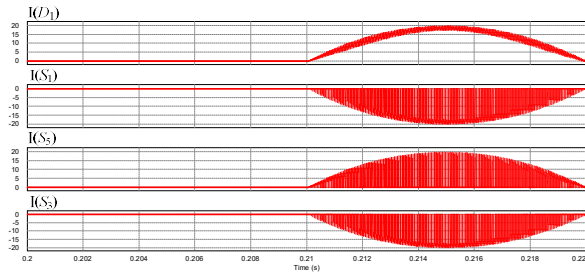
line could also be removed for rectifier mode as Fig.4 (a). In this way, modulation strategies for both modes are different and should be changed with mode transfer. For control simplicity, we choose the same modulation method including some redundancy switching signals.

On the other hand, differences between Fig.4 (a) and Fig.4 (b) are that high frequency switching pulses adopted in  $S_5$  and  $S_6$  for rectifier mode, while line frequency switching pulses adopted in  $S_5$  and  $S_6$  for inverter mode. Corresponding current paths in Tab.1 further illustrate that body diodes are used in rectifier mode while they are not adopted in inverter mode. These two would affect the efficiency of the rectifier mode, which is the inevitable cost with only concise modulation improvement adopted. Fortunately, single H6 inverter solution is suitable for small power fields, where battery storage is adopted for emergency usage. The slightly efficiency decrease is acceptable for practice.

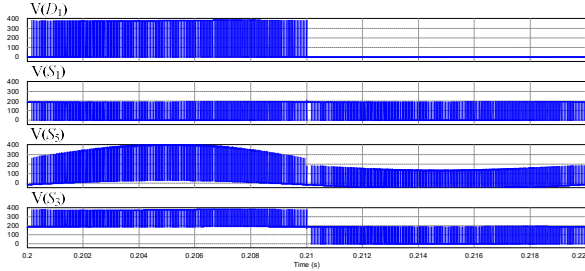
##### C. Bidirectional H6 rectifier/inverter control method

Fig.7 shows the control block of the bidirectional H6 converter. The HV bus voltage  $V_{dc}$  is regulated by the dc bus feedforward voltage loop control. The output current magnitude  $I_{ref}$  is given by the voltage loop. The instantaneous





(a) Current stress



(b) Voltage stress

Figure 9 H6 rectifier device stress

Fig.9 further provides current stress and voltage stress of the main device in the H6 rectifier. Due to the symmetrical structure of the circuit,  $D_1, S_1, S_3, S_5$  are chosen for device selection. It is found that the transient maximum current of them is given by the inductor current with high frequency ripple considered. While the transient maximum voltage of them is clamped to the dc link voltage. Considering the thermal issue and voltage spike, 1.5x-2x current/voltage derating coefficient would be acceptable.

### B. Experimental Test Results



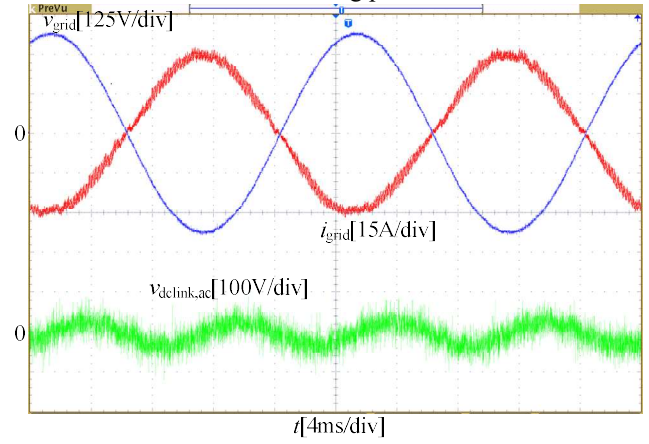
Figure 10 Prototype photograph

Fig.10 further shows the 5kW bidirectional prototype photograph based on H6-topology. Detail test results are provided below.

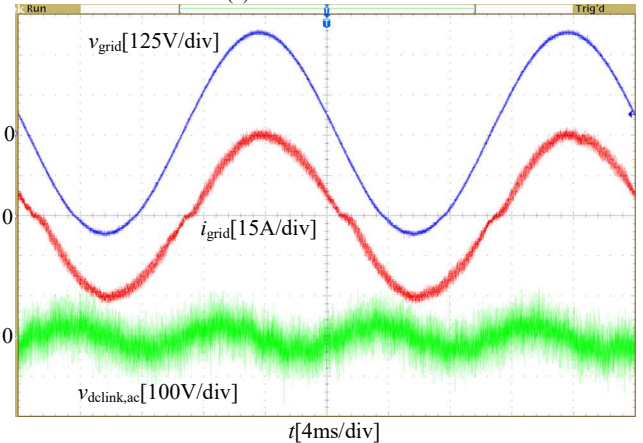
Fig. 11(a) shows that the ac current is of the opposite phase from the ac voltage, while ac current and ac voltage in Fig.11(b) maintain the same frequency, as well as phase. The two curves are typical rectifier and inverter waveform with power factor  $-1$ , and  $1$ , respectively. Double line frequency dc link voltage ripple is also observed in Fig.11, it is a typical single phase system feature. The grid current total harmonic distortion (THD) of the rectifier mode and inverter mode is 3.28% and 2.64%, respectively, which both indicate high grid current performance. However, it is found that there are still

small distortions in zero-crossing points. There are many reasons for zero crossing distortion, e. g. reactive power, dead time, discontinues inductor current mode, modulation methods, impedance with non-ideal loop gain, and etc. And the zero-crossing distortion could be eliminated following the way of [26]-[29] in the future.

Fig. 12 and Fig. 13 illustrate detail gate signals of each active switch. It is found that no matter the converter is a rectifier or inverter, the switching pattern is the same, which

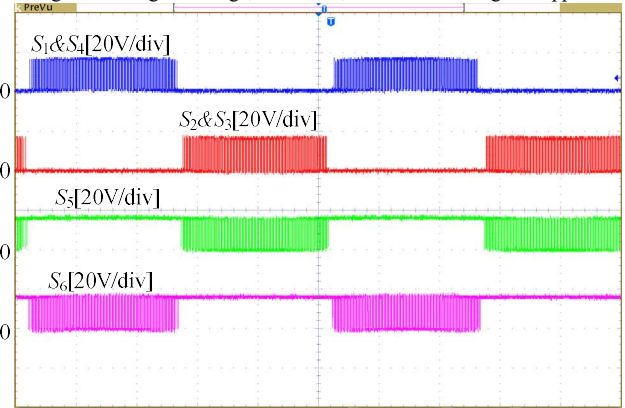


(a) H6 Rectifier Mode

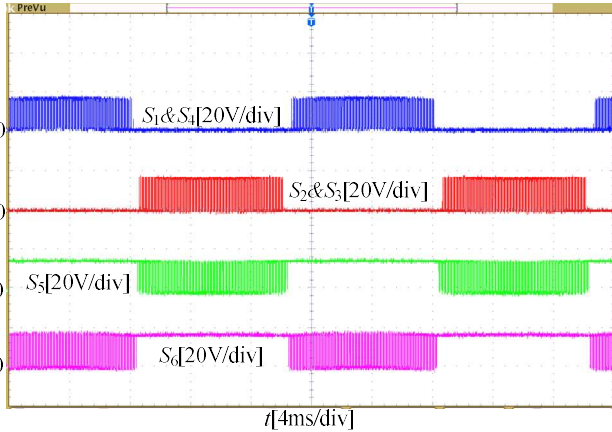


(b) H6 Inverter Mode

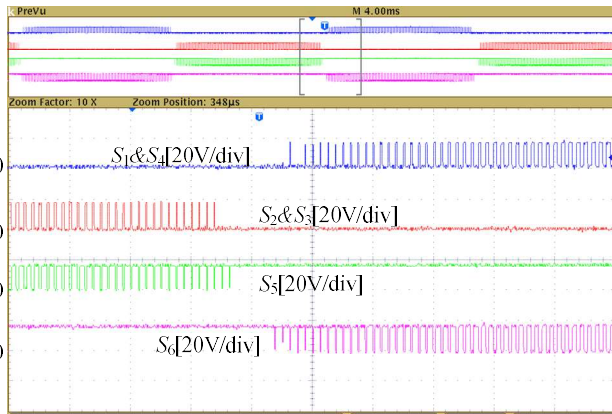
Figure 11 Ac grid voltage, ac current, and dc link voltage ac ripple



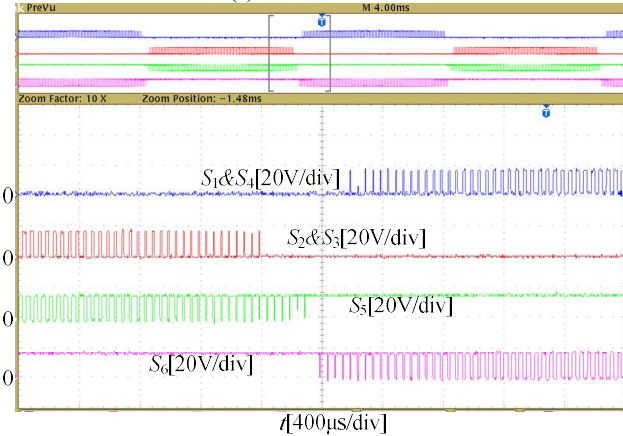
(a) H6 Rectifier Mode



(b) H6 Inverter Mode  
Figure 12 Switching pulses



(a) H6 Rectifier Mode



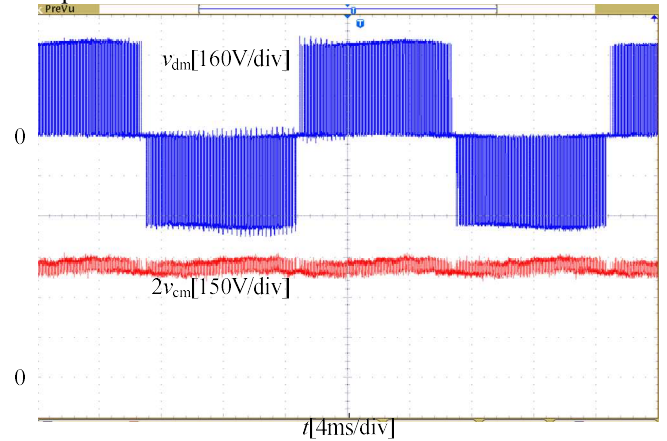
(b) H6 Inverter Mode  
Figure 13 Expanded switching pulses

implies that the same PWM modulation method is adopted as Fig.4 illustrates.

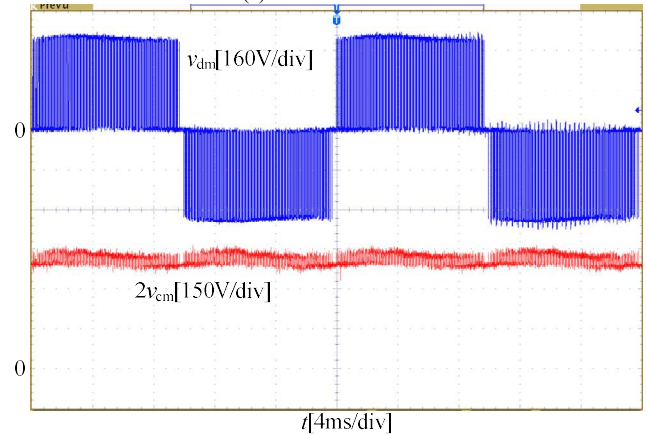
Fig. 14 provides DM voltage and 2xCM voltage of the bidirectional H6 converter. Typical +1, 0, -1 three level voltage shows its DM voltage advantage, while constant dc voltage with small ac ripple verifies excellent CM voltage and leakage current feature as Fig.8 illustrated.

Last but not least, efficiency curve of both rectifier mode and inverter mode are shown in Fig. 15. It is found that the maximum efficiency of the converter in inversion mode is 96.95%, while that in rectifier mode is 96.24% in rectification mode. In rectifier mode, switching two switches with high frequency and using body diodes for power flow paths will definitely increase the switching losses of the converter, compared to the H6 inverter mode. It is the cost for bidirectional power capability like that in bi-polar modulation method and uni-polar modulation method for full bridge inverter. The efficiency of the H6 rectifier slightly lower than H6 inverter.

The most known bidirectional converter is bi-polar modulation single phase full bridge H4 converter. It is proven that H6-type converter is more efficient than bi-polar modulation H4 inverter due to body diode is replaced with extra independent diode at the cost of more devices. Following this way, with more active and passive devices enrolled, dual buck-type converter, three level converters and their derived converters would get more high efficiency but the circuit structures would be more complex. Therefore, considering H6-type converters are the dominant circuits in single phase transformer-less PV applications, the proposed methodology would be regarded as a good trade-off for high cost performance concern.



(a) H6 Rectifier Mode



(b) H6 Inverter Mode



Figure 14 CM voltage, DM voltage( $2 \times \text{CM voltage } 2v_{\text{cm}} = v_{\text{AN}} + v_{\text{BN}}$  measured with oscilloscope math function)

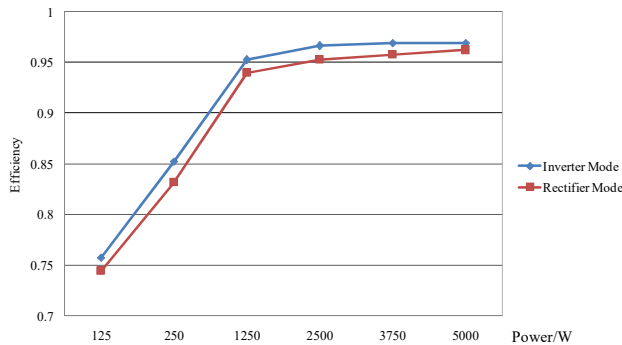


Figure 15 Efficiency curve

## VI. ACKNOWLEDGEMENT

The authors would like to thanks Dr Min Luo from Plexim GmbH for his kindly instruction and help in PLECS RT Box HIL Platform for Power Electronics, which significantly improve our verification work.

## VII. CONCLUSION

Aiming solar energy storage system, this paper improves a grid-tied single phase H6 PV inverter from unidirectional power flow to bidirectional power flow. A unified hybrid modulation method is proposed for both rectifier and inverter modes. The main advantages of the proposed solution can be summarized as:

- 1) Compared with the traditional hybrid modulation method for power rejection to grid only, a simple modification in the switching patterns is just needed for solar energy storage system with H6 type topology.
- 2) Battery storage is adopted for emergency usage in small solar energy storage system. Therefore, a slight cost of efficiency decreases in rectifier mode due to the partly used body diodes is acceptable, and the excellent DM/CM voltage features of the H6 circuitry in both rectifier and inverter modes are totally achieved.
- 3) The improved hybrid modulation method would be easily modified and applied to other H6 and similar topologies.

## VIII. REFERENCE

- [1] R. Teodorescu, M. Liserre, and P. Rodriguez, Grid converters for photovoltaic and wind power systems. Hoboken, NJ, USA: Wiley, 2011.
- [2] Rik W. De Doncker. Power Electronics – key enabling technology for a CO2 neutral electrical energy supply. Available: <http://www.ifecc.tw/rik.html>
- [3] Generators connected to the low-voltage distribution network. Available: <https://www.vde-verlag.de/standards/0105029/vde-ar-n-4105-anwendungsregel-2011-08.html>.
- [4] T. Kerekes, R. Teodorescu, P. Rodriguez, G. Vazquez, and E. Aldabas, "A new high-efficiency single-phase transformerless PV inverter topology," *IEEE Trans. Ind. Electron.*, vol. 58, no. 1, pp. 184-191, 2011.
- [5] R. Bojoi, L. R. Limongi, D. Ruiu, and A. Tenconi, "Enhanced power quality

- control strategy for single-phase inverters in distributed generation systems," *IEEE Trans. Power Electron.*, vol. 26, no. 3, pp. 798-806, 2011.
- [6] M. Yilmaz, P. T. Krein, "Review of the impact of vehicle-to-grid technologies on distribution systems and utility interfaces," *IEEE Trans. Power Electron.*, vol. 28, no. 12, pp. 5673-5689, Dec. 2013.
- [7] B. Ji, J. Wang, J. Zhao, "High-efficiency single-phase transformerless PV H6 inverter with hybrid modulation method," *IEEE Trans. Ind. Electron.* vol.60,no.5,pp.2104-2115,2013.
- [8] L. Zhang, K. Sun, L. Feng, H.Wu, and Y. Xing, "A family of neutral point clamped full-bridge topologies for transformerless photovoltaic grid-tied inverters," *IEEE Trans. Power Electron.*, vol. 28, no. 2, pp. 730-739, 2013.
- [9] W. Li, Y. Gu, H. Luo, et al., "Topology review and derivation methodology of single-phase transformerless photovoltaic inverters for leakage current suppression," *IEEE Trans. Ind. Electron.*, vol. 62, no.7, pp. 45376-4551,2014.
- [10] S. Tan, H. Geng, G. Yang, H. Wang, Blaabjerg, " Modeling framework of voltage-source converters based on equivalence with synchronous generator," *J. Modern Power Syst. Clean Energy*, vol. 6, no. 6, pp. 1291-1305, 2018.
- [11] Y. Yang, F. Blaabjerg, and H. Wang, "Low-voltage ride-through of single-phase transformerless photovoltaic inverters," *IEEE Trans. Ind. Application*, vol. 50, no. 3, pp. 1942-1952, 2014.
- [12] Y. Yang, F. Blaabjerg, "Overview of single-phase grid-connected photovoltaic systems," *Electric Power Components & Systems*, vol. 43, no. 12, pp. 1352-1363, 2015.
- [13] J. Wang, F. Luo, Z. Ji, and etc. , "An improved hybrid modulation method for the single phase H6 inverter with reactive power compensation," *IEEE Trans. Power Electron.*, vol. 33, no. 9, pp. 7674 - 7683, 2018.
- [14] M. Islam, N. Afrin, and S. Mekhilef, "Efficient single phase transformerless inverter for grid-tied PVG system with reactive power control," *IEEE Trans. Sustainable energy*, vol. 7, no. 3, pp. 1205 - 1215, 2016.
- [15] Tsai-Fu Wu, Chia-Ling Kuo, Kun-Han Sun, and Hui-Chung Hsieh, "Combined unipolar and bipolar PWM for current distortion improvement during power compensation," *IEEE Trans. Power Electron.*, vol. 29, no. 4, pp. 1702-1709, 2014.
- [16] T. Freddy, J.H. Lee, H.C. Moon, K. B. Lee, N. Rahim, "Modulation technique for single phase transformerless photovoltaic inverters with reactive power capability," *IEEE Trans. Ind. Electron.*, vol. 64, no. 9, pp. 6989 - 6999, 2017.
- [17] E. Afshari, G. Moradi, A. Ramyar, R. Rahimi, B. Farhangi, S. Farhangi, "Reactive power generation for single-phase transformerless Vehicle-to-Grid inverters: A review and new solutions," in *2017 IEEE Transportation Electrification Conference and Expo (ITEC)*, 2017, pp. 69 - 76.
- [18] H. Qian, J. Zhang, J. -S Lai, et al, "A high-efficiency grid-tie battery energy storage system," *IEEE Trans. Power Electron.*, vol.26, no.3,pp. 886-896, 2011.
- [19] C. Liu, J. Kan, Y. Zhi, et al, "Reliable transformerless battery energy storage systems based on cascade dual-boost/buck converters," *IET Power Electron.*, vol.8,no.9,pp.1681-1689, 2015.
- [20] B. Gu, J. Dominic, J.-S. Lai, C.-L. Chen, T. LaBella, and B. Chen, "High reliability and efficiency single-phase transformerless inverter for grid-connected photovoltaic systems," *IEEE Trans. Power Electron.*, vol. 28,no. 5, pp. 2235-2245, 2013.
- [21] C. Liu, Y. Wang, J. Cui, et al., "Transformerless photovoltaic inverter based on interleaving high-frequency legs having bidirectional capability," *IEEE Trans. Power Electron.*, vol. 31, no. 2, pp. 1131-1142, 2016.
- [22] Temesi Ernő and Michael Frisch, 2nd generation of PFC solutions. Available: <https://www.vincotech.com/support-and-documents/technical-library.html>
- [23] Michael Frisch and Temesi Ernő, High efficient topologies for next generation solar inverter. Available: <https://www.vincotech.com/support-and-documents/technical-library.html>
- [24] S. Acaujo, P. Zacharias, and R. Mallwitz, "Highly efficient single-phase transformerless inverters for grid-connected photovoltaic systems," *IEEE Trans. Ind. Electron.*, vol. 57, no. 9, pp.3118 - 3128, 2010.
- [25] L. Huber, Y. Jang, and M. M. Jovanovic, "Performance evaluation of bridgeless PFC boost rectifiers," *IEEE Trans. Power Electron.*, vol. 23, no. 3, pp. 1381-1390, 2008.
- [26] Jian Sun, "On the zero-crossing distortion in single-phase PFC converters," *IEEE Trans. Power Electron.*, vol. 19, no. 3, pp. 685 - 692, 2004.
- [27] Jian Sun, "Input impedance analysis of single-phase PFC converters," *IEEE Trans. Power Electron.*, vol. 20, no. 2, pp. 308-314, 2005.
- [28] B. Liu, M. Su, J. Yang, D. Song, D. He, S. Song, "Combined reactive power injection modulation and grid current distortion improvement approach for H6 transformer-less photovoltaic inverter", *IEEE Trans. Energy Conversion*, vol. 32, no. 4, pp. 1456 - 1467, 2017.
- [29] P. Sun, C. Liu, J. S. Lai, C.L. Chen, "Cascade dual buck inverter with phase-shift control", *IEEE Trans. Power Electron.*, vol. 27, no. 4, pp. 2067 - 2077, 2012.

**Jianhua Wang (M'11)** received the B.S. and Ph.D. degrees in electrical engineering from Nanjing University of Aeronautics & Astronautics, Nanjing, China, in 2004 and 2010, respectively.



In 2010, he joined the Faculty of School of Electrical Engineering in Southeast University, Nanjing, China, where he is currently an Associate Research Professor. He has published more than 40 technical papers. He is the holder of 3 China patents. His main research interests are MVDC, solid-state transformer, power electronics system stability, distributed generation and micro-grid.

**Shang Gao** received the B.S. degree from Shandong University, Jinan, China, in 2017. Currently he is pursuing the M.S. degree at Southeast University, Nanjing, China. His main research interests are MVDC, and power electronics system stability.



**Yichao Sun (S'13–M'17)** received the B.S. and Ph.D. degrees in electrical engineering from Southeast University, Nanjing, China, in 2010 and 2017, respectively.



From February 2015 to August 2016, he was a Visiting Scholar in the Power Electronics Group (PEG), RMIT University, Melbourne, Vic., Australia. Since 2017, he joined School of Electrical and Automation Engineering, Nanjing Normal University, Nanjing, China, where he is currently a Lecturer. His current research interests include the modulation and control of power electronic converters, with a particular emphasis on multilevel converters.

**Zhendong Ji** received the B.S. and Ph.D. degrees in electrical engineering from Southeast University, Nanjing, China, in 2007 and 2015, respectively.



Since 2015, he joined the School of Automation in Nanjing University of Science and Technology, Nanjing, China, where he is currently a Lecturer. His main research interests include cascade multilevel converters and solid-state transformers.

**Lexiang Cheng** received the B.S. degree from Nanjing university of Science and Technology, Nanjing, China, in 2007 and the M.E. degree from Southeast University, Nanjing, China, in 2010.



Since 2010, he joined State Grid Nanjing Power Supply Company, Nanjing, China. His main research interests include integration techniques of distributed generation and renewable energy sources.

**Lingyu Li** received the B.S. degree in applied physics from Hohai University and the M.S. degree in electrical engineering from Southeast University Nanjing, China, in 2008 and 2016, respectively.



Since 2016, she joined in State Grid Yancheng Power Supply Company, Yancheng, China, where she is currently an electrical engineer. Her main research interests are distributed generation, and substation operation and maintenance.

**Wei Gu (M'06–SM'16)** received his B. Eng degree and Ph.D. degree in Electrical Engineering from Southeast University, China, in 2001 and 2006.



From 2009 to 2010, he was a Visiting Scholar in the Department of Electrical Engineering, Arizona State University, Tempe, AZ 85287, USA. He is now a Professor in School of Electrical Engineering, Southeast University. His research interests are power system stability and control, smart grid, renewable energy technology and power quality.

**Jianfeng Zhao** received the B.S. from Huainan Mining Institute, Huainan, China, the M.S. degree from Nanjing University of Aeronautics & Astronautics, Nanjing, China, and the Ph.D. degrees from Southeast University, Nanjing, China, in 1995, 1998, and 2001, respectively, all in electrical engineering.



In 2001, he joined the Faculty of School of Electrical Engineering, Southeast University, where since 2008 he has been a Professor and has been engaged in teaching and research in the field of high-power power electronics. Since 2014, he has also been the Dean of School of Electrical Engineering, Southeast University. He has authored or coauthored more than 100 technical papers. He holds more than 50 China patents. His current research interests include utility applications of power electronics in smart grid such as solid-state transformer, active filters for power conditioning, flexible ac-transmission system devices, multilevel ac-motor drives, and efficient energy utilization.